Journal of Molecular Structure 892 (2008) 116–120

Contents lists available at ScienceDirect

Journal of Molecular Structure

journal homepage: www.elsevier.com/locate/molstruc

Study on the interaction between bovine serum albumin and CdTe quantum dots with spectroscopic techniques

Jiangong Liang, Yanping Cheng, Heyou Han *

College of Science, State Key Laboratory of Agricultural Microbiology, Institute of Chemical Biology, Huazhong Agricultural University, Wuhan 430070, People's Republic of China

ARTICLE INFO

Article history:
Received 26 March 2008
Accepted 5 May 2008
Available online 11 May 2008

Keywords:
CdTe quantum dots
Bovine serum albumin
Interaction
Spectroscopic techniques

ABSTRACT

The interaction between bovine serum albumin (BSA) and CdTe quantum dots (QDs) was studied by fluorescence, UV–vis and Raman spectroscopic techniques. The results showed that the fluorescence of BSA was strongly quenched by CdTe QDs. The quenching mechanism was discussed to be a static quenching procedure, which was proved by the quenching rate constant (K_q) and UV–vis absorption spectra. According to Lineweaver–Burk equations at different temperatures, the thermodynamic parameters, ΔH^{θ}, ΔS^{θ} and ΔG^{θ} were observed to be -23.69 kJ mol^{-1}, 48.39 J mol^{-1} K^{-1} and -38.04 kJ mol^{-1}, respectively. The binding constant (K_A) and the number of binding sites (n) were obtained by Scatchard equation. It was found that hydrophobic force and sulfhydryl group played a key role in the interaction process. Further results from Raman spectra indicated that the α-helical content in BSA reduced after binding with CdTe QDs.

1. Introduction

Luminescent quantum dots (QDs) have been widely used as a novel fluorescent probe in biosensor and bioimaging due to their unique optical and electrical properties [1–3]. Bovine serum albumin (BSA) has been one of the most extensively studied proteins, particularly because of its structural homology with human serum albumin [4]. The BSA molecule is made up of three homologous domains (I, II, and III) which are divided into nine loops (L1–L9) by 17 disulfide bonds [5]. BSA has two tryptophans, Trp-134 and Trp-212, that possess intrinsic fluorescence, embedded in the first subdomain IB and subdomain IIA, respectively [4]. BSA was often used as coating reagent to modify the surface of nanoparticles due to its strong affinity to a variety of nanoparticles, such as gold nanoparticles [6], silica nanoparticles [7], and QDs [8,9]. Up to now, QDs modified by BSA have been applied to ion sensors [10–12], fluorescence resonance energy transfer [13,14], and chemiluminescence resonance energy transfer [15]. However, the mechanism of interaction between BSA and QDs has not yet been determined, which was often thought as electrostatic attraction [9,15].

This work reports investigations aiming at verifying the occurrence of specific interaction between BSA and CdTe QDs. We investigated the interaction between BSA and CdTe QDs according to the effect of CdTe QDs on the fluorescence of BSA with spectroscopic techniques. It was found that the fluorescence of BSA was strongly quenched by CdTe QDs. A static quenching procedure was proved by the quenching rate constant (K_q) and UV–vis absorption spectra. Lineweaver–Burk equation was used to calculate the thermodynamic parameters, ΔH^{θ}, ΔS^{θ} and ΔG^{θ} in the quenching process. The mechanism of interaction was also discussed, which showed that hydrophobic force and sulfhydryl group play an important role in the quenching process.

2. Experimental

2.1. Apparatus

The UV–vis absorption spectra were obtained with 1.0 cm × 1.0 cm-quartz cuvette on a Thermo Nicolet Corporation Model evolution 300 (America). All fluorescence spectra were recorded by a Perkin-Elmer LS-55 fluorescence spectrometer (America) equipped with a 20 kW xenon discharge lamp as a light source. The Raman spectra were acquired with an inVia micro-Raman spectroscopy system (Renishow, UK) in a spectral range of 300–2000 cm^{-1}, equipped with a He–Ne laser excitation source emitting wavelength at 633 nm. And all pH measurements were made with a Model pHS-3C meter (Shanghai Leici Equipment Factory, China).

2.2. Chemicals

Tellurium powder (99.99%), $CdCl_2{\cdot}2.5H_2O$ (99.0%) and $NaBH_4$ (96%) were obtained from Tianjin Chemical Reagent Plant (Tianjin, China). Thioglycolic acid (TGA) was obtained from Shanghai Chem-

* Corresponding author. Tel./fax: +86 27 87288246.
E-mail address: hyhan@mail.hzau.edu.cn (H. Han).

0022-2860/$ - see front matter © 2008 Published by Elsevier B.V.
doi:10.1016/j.molstruc.2008.05.005

ical Reagent Co., Ltd. (Shanghai, China). And BSA was purchased from Shanghai Boao Biochemical Technology Co. (Shanghai, China,). All other chemicals were of analytical grade and were used without further purification.

2.3. The synthesis and purification of CdTe QDs

Thiol-capped CdTe QDs were synthesized following the method reported by Zhang et al. with some modifications [16]. Briefly, 80 mg of sodium borohydride, 127.5 mg of tellurium powder and 1.00 mL of ultrapure water were transferred to a small flask, and the reacting system was cooled in an ice-water bath. After 8 h reaction, the black tellurium powder disappeared and sodium tetraborate white precipitation appeared on the bottom of the flask. The resulting NaHTe in clear supernatant was separated and added to $CdCl_2$ solution in the presence of TGA at N_2 atmosphere. The molar ratio of Cd^{2+}:Te^{2-}:TGA was fixed at 1:0.5:2.4. After mixing, the solution was heated to 100 °C, and thiol-capped CdTe QDs could be obtained. The CdTe QD sizes could be controlled simply by varying the reaction time from 0.2 to 10 h. The resulting products were precipitated by acetone, and superfluous TGA and Cd^{2+} that did not participate in the reaction were removed with centrifugation at 4000 rpm for 3 min. The resultant precipitate was re-dispersed in water, and re-precipitated by an amount of acetone for more than two times, then kept at 4 °C in dark for further use.

2.4. Preparation of denatured bovine serum albumin (dBSA)

dBSA was prepared by chemically treating BSA with $NaBH_4$ according to the method reported by references [9,17]. BSA (0.165 g) was dissolved in 50 mL of deionized water, and then 0.0042 g of $NaBH_4$ was added as a reductant into the solution under stirring. The reaction proceeded at room temperature for 1 h and excess borohydride was removed by spontaneous decomposition upon heating. Under these conditions, BSA was denatured and most of its disulfide bonds were converted to sulfhydryl groups. The final concentration of dBSA aqueous solution was 5.0×10^{-5} M [9,17].

2.5. The effect of CdTe QDs on the fluorescence of BSA

BSA concentration was kept fixed at 1.0×10^{-6} M and QD concentration was varied from 0 to 1.5×10^{-6} M. Fluorescence spectra were recorded at 298 and 313 K in the range of 300–500 nm upon excitation at 280 nm in each case.

2.6. The determination of binding parameters

To analyze the interaction between BSA and CdTe QDs, the quenching constant of protein fluorescence K'_{SV} was determined from the Stern–Volmer equation modified by Lehrer [18]:

$$F_0/(F_0 - F) = 1/f_a + 1/([Q]f_a K'_{SV}) \quad (1)$$

where, F_0 and F are the relative fluorescence of BSA in the absence and presence of quencher [Q] (CdTe QDs), respectively. f_a is the fractional maximum fluorescence intensity of BSA, K'_{SV} is the quenching constant, and [Q] is the CdTe QD concentration. The binding constant (K_A) and the number of binding sites (n) were determined by the use of Scatchard method [19]:

$$\lg[(F_0 - F)/F] = \lg K_A + n \lg[Q] \quad (2)$$

In the formula (2), n is the number of binding sites, and K_A is the binding constant for the QD–BSA complex.

2.7. Calculation of thermodynamic parameters, ΔH^θ, ΔS^θ and ΔG^θ

The determination of the change of free enthalpy based on the van't Hoff equation:

$$\Delta G^\theta = -RT \ln K \quad (3)$$

where, R is the gas constant 8.314 J mol^{-1} K^{-1} and T is the temperature (K). K is the equilibrium constant at the corresponding temperature, which stands for static quenching constant in the present paper. The enthalpy change (ΔH^θ) and entropy change (ΔS^θ) can be calculated from the following equations:

$$\ln K_2^\theta / K_1^\theta = [1/T_1 - 1/T_2]\Delta H^\theta / R \quad (4)$$

$$\Delta G^\theta = \Delta H^\theta - T\Delta S^\theta \quad (5)$$

3. Results and discussion

3.1. Characterization of as-prepared CdTe QDs

Fig. 1 depicted the UV–vis absorption spectra of four sizes of CdTe QDs. The UV–vis absorption edge of CdTe QDs showed an obvious blue-shift from bulk band gap of 827 nm, indicating the effect of quantum confinement [20]. A well-resolved absorption maximum of the first electronic transition is observed and showed a narrow size distribution of the CdTe QDs. The particles sizes of CdTe QDs were determined from the first absorption maximum of the UV–vis absorption spectra according to the following formula [21]:

$$D = (9.8127 \times 10^{-7})\lambda^3 - (1.7147 \times 10^{-3})\lambda^2 + (1.0064)\lambda - 194.84 \quad (6)$$

where D (nm) is the size of a given CdTe QD sample, and λ (nm) is the wavelength of the first excitonic absorption peak of the corresponding sample. The results showed that the particle diameters of the as-prepared CdTe QDs were around 1.8, 2.6, 3.1 and 3.4 nm, corresponding with the first absorption maximum of 483, 510, 540 and 562 nm, respectively.

The concentrations of CdTe QDs were calculated by using Lambert-Beer's law:

$$A = \varepsilon CL \quad (7)$$

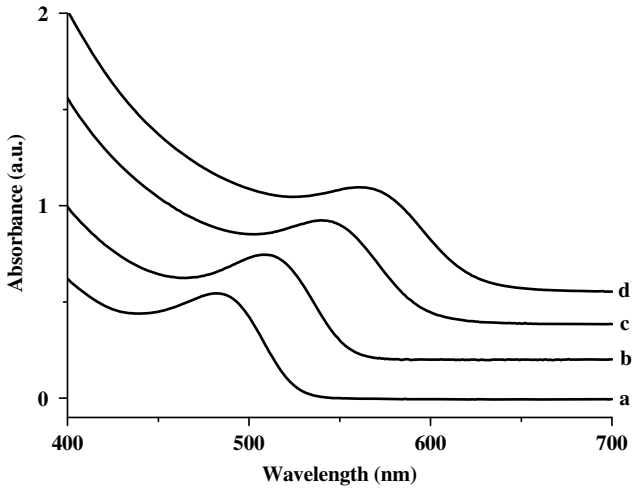

Fig. 1. UV–vis absorption spectra of different size of CdTe QDs. The average diameters of the QDs are (a) 1.8 nm, (b) 2.6 nm (c) 3.1 nm and (d) 3.4 nm, which were estimated from their corresponding UV–vis absorption peaks.

In the above equation, A is the absorbance at the peak position of the first excitonic absorption peak for a given sample. C (M) is the molar concentration of the CdTe QDs of the same sample. L (cm) is the path length of the radiation beam used for recording the absorption spectrum, and ε (M^{-1} cm^{-1}) is the extinction coefficient per mole of CdTe QDs at the first exitonic absorption peak, which could be obtained from formula $\varepsilon = 10{,}043\ (D)^{2.12}$ [21].

3.2. Fluorescence quenching spectra

The effect of CdTe QDs on BSA fluorescence intensity is shown in Fig. 2. When different amounts of CdTe QD solution were added to a fixed concentration of BSA, a remarkable decrease in the fluorescence intensity of BSA was observed and indicated an interaction between BSA and CdTe QDs. The fluorescence quenching data were analyzed by the Stern–Volmer equation,

$$F_0/F = 1 + K_{SV}[Q] \quad (8)$$

where F_0 and F are the fluorescence intensities of BSA in the absence and presence of CdTe QDs, respectively, K_{SV} is the Stern–Volmer quenching constant and [Q] is the concentration of QDs. The plot of F_0/F versus [Q] (Fig. 3) showed a positive deviation (concave towards the y axis), indicating the presence of both static and dynamic quenching [22]. The fluorescence data obtained at 298 K were further examined using modified Stern–Volmer equation (Formula (1)). From the plot of $F_0/(F_0 - F)$ versus 1/[Q], the values of f_a and K'_{SV} were obtained from the values of intercept and slope, respectively (Fig. 4). The value of f_a was observed to be 1.19 at 298 K, showing that 84.0% of the total fluorescence of BSA is accessible to the quencher (QDs). The K'_{SV} was found to be $5.87 \times 10^6\ M^{-1}$. Since the fluorescence lifetime of the biopolymer is 10^{-8} s [23], the quenching rate constant, K_q, could be calculated according to equation $K_q = K'_{SV}/\tau_0$. This K_q value was observed to be $5.87 \times 10^{14}\ M^{-1}\ s^{-1}$ at 298 K. The quench constants are greater than those in the biopolymer ($2.0 \times 10^{10}\ M^{-1}\ s^{-1}$) by the maximum scatter collision mechanism [24]. It means that the quenching is not initiated by dynamic collision but by the formation of a complex, namely static quenching.

UV–vis absorption measurement is a very simple method and applicable to explore the structural changes and to know the complex formation [25]. In the present study, we have recorded the UV-vis absorption spectra of BSA (Fig. 5a), QDs (Fig. 5c) and BSA–QD (Fig. 5b) system. When the BSA was added, the absorption spectrum was different from the result of the single spectra addition of CdTe QDs and BSA (Fig. 5d). On the contrary, the absorption intensity decreased severely at the wavelength of 220 nm. The results indicated that the binding between CdTe QDs and protein molecule may lead to a change in BSA conformation.

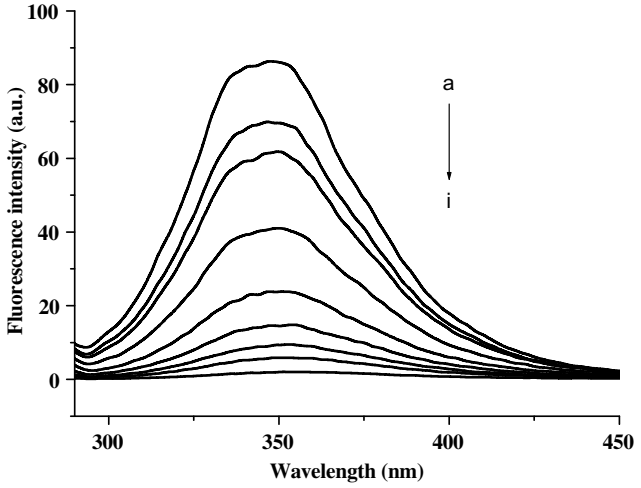

Fig. 2. (a) Fluorescence spectra of BSA in the presence of 2.6 nm CdTe QDs at 0.1 M pH 7.4 Tris–HCl buffer. BSA concentration was fixed at 1.0×10^{-6} M. CdTe QD concentrations were (a) 0, (b) 0.5, (c) 1.0, (d) 2.0, (e) 4.0, (f) 6.0, (g) 8.0, (h) 10.0, (i) 15.0×10^{-7} M.

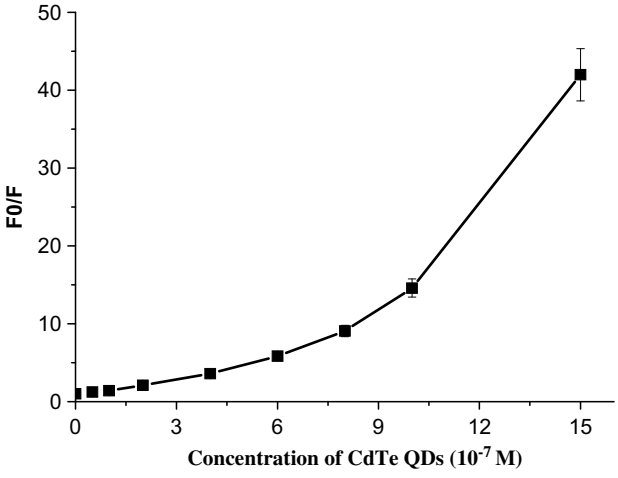

Fig. 3. Unmodified Stern–Volmer curves of F_0/F vs concentration of 2.6 nm CdTe QDs at 298 K at 0.1 M pH 7.4 Tris–HCl buffer. The concentration of BSA was 1.0×10^{-6} M.

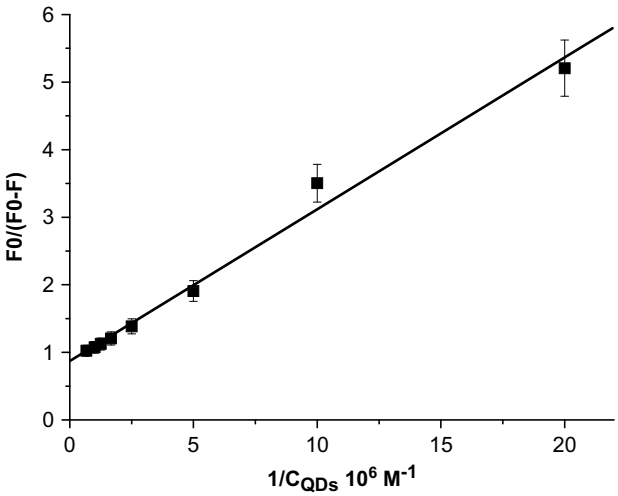

Fig. 4. Modified Stern–Volmer curves of $F_0/(F_0 - F)$ vs concentration of 2.6 nm CdTe QDs at 298 K at 0.1 M pH 7.4 Tris–HCl buffer. The concentration of BSA was 1.0×10^{-6} M.

3.3. Thermodynamic parameters and binding mode

The static quenching constant (K) of BSA with CdTe QDs could be calculated by employing the Lineweaver–Burk equation [26]:

$$1/(F_0 - F) = 1/F_0 + 1/(KF_0[Q]) \quad (9)$$

The interaction studies were carried out at 298, 306 and 313 K. The values of K, ΔH^θ, ΔS^θ and ΔG^θ were summarized in Table 1. The negative value of ΔG^θ revealed that the interaction process is spontaneous. The positive entropy change occurs because the water molecules which are arranged in an orderly fashion around the QDs and BSA, acquired the more random configuration as a result of hydrophobic interaction [27].

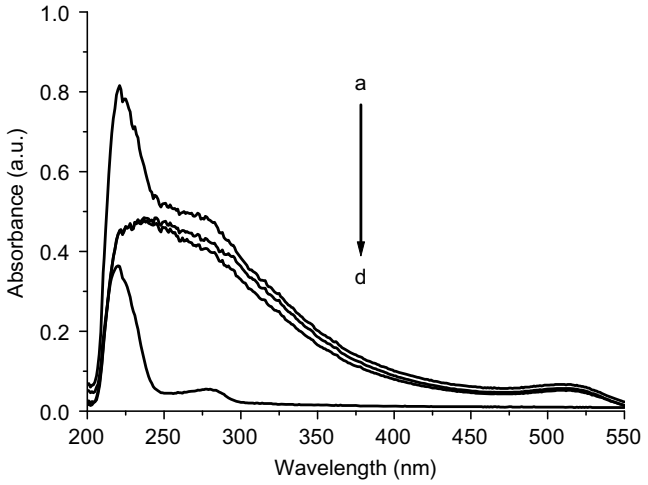

Fig. 5. The UV–vis absorption spectra of (a) the sum of CdTe QDs and BSA, (b) CdTe QDs, (c) BSA–CdTe QDs and (d) BSA. The concentration of CdSe QDs and BSA were 1.0×10^{-6} M. The size of CdTe QDs was 2.6 nm.

Table 1
Binding constants (K) and thermodynamic parameters for interaction of BSA with 2.6 nm CdTe QDs

Temperature (K)	K_A (M^{-1})	n	K ($\times 10^6$ M^{-1})	ΔG^θ (kJ mol^{-1})	ΔH^θ (kJ mol^{-1})	ΔS^θ (J mol^{-1} K^{-1})
298	1.21×10^9	1.34	4.65	−38.04	−23.69	48.39
306	5.13×10^9	1.44	4.11	−38.74		
313	1.23×10^{11}	1.65	2.83	−38.66		

The Scatchard method has been used to get the number of binding sites (n) and the binding constant (K_A). The number of QDs n = 1.3–1.7 per molecule of BSA is determined. The value increases with rise of temperature (Table 1) probably due to slight changes of the protein structure. This not only results in the exposition of the hydrophobic residue but also does in easier access of the CdTe QDs to the binding sites of BSA [27].

3.4. The effect of QD size on the interaction

The size of QDs plays an important role in the interaction of CdTe QDs with BSA. As shown in Table 2, K_A increased with the increase of QD size. The number of QD n = 1.1–1.5 per molecule of BSA was determined. The obtained values were increased with the decrease of QD size (Table 2) probably due to the changes of relative size between BSA and CdTe QDs [19].

3.5. The interaction mechanism

Fluorescence quenching can result from a variety of molecular interactions, including excited-state reactions, molecular rearrangements, energy transfer, ground-state complex formation, and collisional quenching [28]. According to the above results and some literatures [15,29], a static quenching mechanism for the interaction of BSA with CdTe QDs is suggested, which may result from the electrostatic interaction, hydrophobic force, as well as sulfhydryl group.

The change of ionic strength is an efficient method for distinguishing the binding modes between protein and other molecules. The high ionic strength was advantageous to the hydrophobic process but disadvantageous to the electrostatic binding [30]. Fig. 6 showed the effect of NaCl concentration on the interaction of BSA with CdTe QDs. The experimental results showed that the concentration of NaCl had little effect on the interaction of BSA with CdTe QDs. The isoelectric point of BSA is 4.6, and therefore BSA is negatively charged at pH 7.4 Tris–HCl buffers [6]. CdTe QDs modified with TGA is also negatively charged at pH 7.4. It indicates the electrostatic force is very weak in the interaction between BSA and CdTe QDs.

Chemically reduced BSA has been used to modify the surface of water-soluble CdTe QDs and CdSe/ZnS QDs, which demonstrate that the dBSA could be conjugated to the surface of QDs and efficiently improve the chemical stability and the fluorescence quantum yield of the QDs [9,17]. For further investigation of the interaction of BSA and CdTe QDs, the disulfide bonds of BSA were converted to sulfhydryl groups using $NaBH_4$ as reductant. Table 2 indicates the Scatchard equations of interaction between BSA, dBSA and CdTe QDs, respectively. The value of binding number of 3.1 nm QDs with dBSA is 1.51 per molecule of dBSA, which is higher than that of normal BSA with 3.1 nm CdTe QDs (1.31). The binding constant (K_A) is also higher than that of normal BSA. This means that sulfhydryl groups play an important role in the interaction of BSA with CdTe QDs.

Raman spectrum is a good tool to study the interaction of protein and nanoparticles [29]. Fig. 7 depicts the Raman spectra of BSA before (Fig. 7a) and after (Fig. 7b) binding to the surface of CdTe QDs. The 1653 cm^{-1} band mainly contribution from amide I, are characteristic of high α-helical content in BSA. The intensity decrease at 1653 cm^{-1} indicates that the α-helical content in BSA was reduced after binding to CdTe QDs [31]. The 1002 cm^{-1} band related to the phenylalanine and 1345 cm^{-1} band related to tryptophan or C–H bending was decreased after BSA interaction with CdTe QDs at 1:1 ratio, showing the exposure of hydrophobic groups of BSA [31]. Thus, the presence of CdTe QDs could result in structural alterations in the BSA conformation and the exposure of hydrophobic groups.

Table 2
Scatchard equations of interaction between BSA, dBSA and CdTe QDs

Size of CdTe QDs (nm)	Equation	R^2	K_A (M^{-1})	n
1.8	$Y = 1.47X + 9.12$	0.998	1.23×10^9	1.47
2.6	$Y = 1.34X + 9.082$	0.985	1.21×10^9	1.34
3.1	$Y = 1.31X + 9.12$	0.984	1.32×10^9	1.31
3.4	$Y = 1.27X + 8.92$	0.996	8.31×10^8	1.27
3.1*	$Y = 1.51X + 11.03$	0.992	1.07×10^{11}	1.51

* The interaction between dBSA and CdTe QDs.

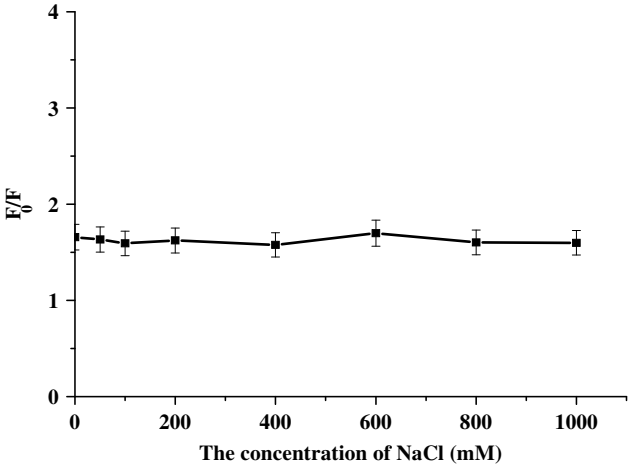

Fig. 6. Effect of NaCl on the fluorescence intensity of BSA and BSA–QDs at 0.1 M pH 7.4 Tris–HCl buffer. The concentrations of BSA and 3.1 nm CdTe QDs were 1.0×10^{-6} M and 1.0×10^{-7} M, respectively.

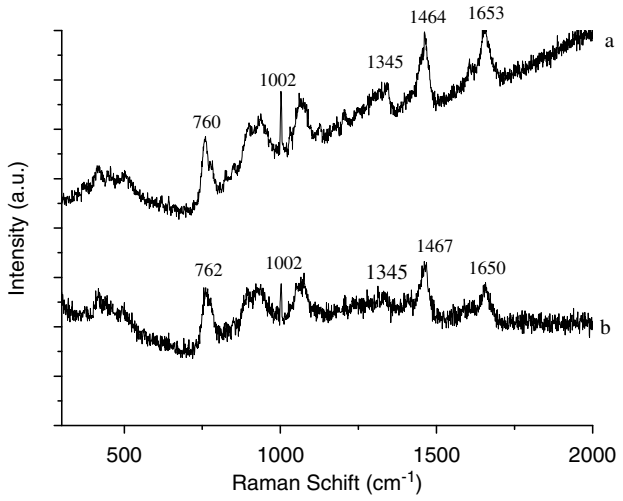

Fig. 7. Raman spectra of BSA before (a) and after (b) adding 1.8 nm CdTe QDs. The concentrations of BSA and CdTe QDs were 2.0×10^{-4} M.

4. Conclusions

In this article, we investigated the interaction between BSA and CdTe QDs with spectroscopic techniques. It was found that the fluorescence of BSA was quenched by CdTe QDs at pH 7.4. A static quenching model based on the quenching rate constant (K_q) and UV–vis absorption spectra was proved. The thermodynamic parameters, ΔH^{θ}, ΔS^{θ} and ΔG^{θ}, were obtained to be -23.69 kJ mol^{-1}, 48.39 J mol^{-1} K^{-1}, -38.04 kJ mol^{-1} according to Lineweaver–Burk equation at different temperatures. Scatchard equation was used to calculate binding constant (K_A) and the number of binding sites (n). The interaction mechanism was also discussed. It was found that hydrophobic force and sulfhydryl group play an important role in the quenching process. Further results from Raman spectra showed some structural changes of BSA after interaction with CdTe QDs.

Acknowledgments

The authors gratefully acknowledge the support for this research by National Natural Science Foundation of China (20675034), Program for New Century Excellent Talents in Chinese Ministry of Education (NCET-05-0668), Key Project of Chinese Ministry of Education (106120), Nature Science Foundation from Hubei Province of China (2006ABA160) and Project Sponsored by the Scientific Research Foundation of Huazhong Agricultural University (2006XRC025).

References

[1] M. Bruchez Jr., M. Moronne, P. Gin, S. Weiss, A.P. Alivisatos, Science 281 (1998) 2013–2015.
[2] W.C.W. Chan, S. Nie, Science 281 (1998) 2016–2018.
[3] X. Michalet, F.F. Pinaud, L.A. Bentolila, J.M. Tsay, S. Doose, J.J. Li, G. Sundaresan, A.M. Wu, S.S. Gambhir, S. Weiss, Science 307 (2005) 538–544.
[4] K. Yamasaki, T. Maruyama, U. Kragh-Hansen, M. Otagiri, Biochim. Biophys. Acta 1295 (1996) 147–157.
[5] G.L. Friedli, Ph.D. Thesis, University of Surrey, 1996.
[6] S.H. Brewer, W.R. Glomm, M.C. Johnson, M.K. Knag, S. Franzen, Langmuir 21 (2005) 9303–9307.
[7] M. Lundqvist, I. Sethson, B.H. Jonsson, Langmuir 20 (2004) 10639–10647.
[8] W.C.W. Chan, Ph.D. Thesis, Indiana University, 2001.
[9] X.H. Gao, W.C.W. Chan, S.M. Nie, J. Biomed. Opt. 7 (2002) 532–537.
[10] J.G. Liang, X.P. Ai, Z.K. He, D.W. Pang, Analyst 129 (2004) 619–622.
[11] J.H. Wang, H.Q. Wang, H.L. Zhang, X.Q. Li, X.F. Hua, Y.C. Cao, Z.L. Huang, Y.D. Zhao, Anal. Bioanal. Chem. 388 (2007) 969–974.
[12] H.Y. Xie, J.G. Liang, Z.L. Zhang, Y. Liu, Z.K. He, D.W. Pang, Spectrochim. Acta A 60 (2004) 2527–2530.
[13] N.N. Mameova, N.A. Kotov, A.L. Rogach, Nano Lett. 1 (2001) 281–286.
[14] D.M. Willard, L.L. Carillo, J. Jung, A. Van Orden, Nano Lett. 1 (2001) 469–474.
[15] X. Huang, L. Li, H. Qian, C. Dong, J. Ren, Angew. Chem. Int. Ed. 45 (2006) 5140–5143.
[16] H. Zhang, Z. Zhou, B. Yang, M.Y. Gao, J. Phys. Chem. B 107 (2003) 8–13.
[17] Q. Wang, Y. Kuo, Y. Wang, G. Shin, C. Ruengruglikit, Q. Huang, J. Phys. Chem. B 110 (2006) 16860–16866.
[18] M.R. Eftink, C.A. Ghiron, Biochemistry 15 (1976) 672–680.
[19] T. Hiratsuka, J. Biol. Chem. 265 (1990) 18786–18790.
[20] C.B. Murray, D.J. Norris, M.G. Bawendi, J. Am. Chem. Soc. 115 (1993) 8706–8715.
[21] W.W. Yu, L.H. Qu, W.Z. Guo, X.G. Peng, Chem. Mater. 15 (2003) 2854–2860.
[22] S.M.T. Shaikh, J. Seetharamappa, S. Ashoka, P.B. Kandagal, Dyes Pigm. 73 (2007) 211–216.
[23] G.Z. Chen, X.Z. Huang, J.G. Xu, Z.Z. Zheng, Z.B. Wang, The Methods of Fluorescence Analysis, second ed., Beijing Science Press, Beijing, 1990 (Chapter 1).
[24] W.R. Ware, J. Phys. Chem. 66 (1962) 445–453.
[25] P.B. Kandagal, J. Seetharamappa, S. Ashoka, S.M.T. Shaikh, D.H. Manjunatha, Int. J. Biol. Macromol. 39 (2006) 234–239.
[26] J.N. Tian, J.Q. Liu, W.Y. He, Z.D. Hu, X.J. Yao, X.G. Chen, Biomacromolecules 5 (2004) 1956–1961.
[27] A. Sułkowska, M. Maciążek, J. Równicka, B. Bojko, D. Pentak, W.W. Sułkowski, J. Mol. Struct. 834–836 (2007) 162–169.
[28] S.M.T. Shaikh, J. Seetharamappa, P.B. Kandagal, S. Ashoka, J. Mol. Struct. 786 (2006) 46–52.
[29] X.C. Shen, X.Y. Liou, L.P. Ye, H. Liang, Z.Y. Wang, J. Colloid Interface Sci. 311 (2007) 400–406.
[30] D.E. Otzen, Biophys. J. 83 (2002) 2219–2230.
[31] G. Meng, J.C.K. Chan, D. Rousseau, E.C.Y. Li-Chan, J. Agric. Food Chem. 53 (2005) 845–852.